# Bidirectional inventory control with optimal use of intermediate storage

Cristina Zotică[a], Krister Forsman[b], Sigurd Skogestad[a,]

[a]*Department of Chemical Engineering, Norwegian University of Science and Technology (NTNU), 7491, Trondheim, Norway*
[b]*Perstorp Specialty Chemicals, 284 80, Perstorp, Sweden*

**Abstract**

The scope of this work is to advocate the use of a decentralized control system that is able to maximize production when temporary or permanent bottlenecks occur for multiple units in series by employing the buffer inventories at intermediate storage. This bidirectional inventory control scheme has for each inventory two controllers, one for the inflow and one for the outflow, with high and low inventory setpoints, respectively. The inventory can typically be liquid (level) or gas (pressure). When production cannot be maintained without breaching physical constraints on the inventory, this control structure automatically reconfigures the loops for consistent inventory control, which means that it is radiating around the throughput manipulator to assure local consistency and feasible operation.

*Keywords:* Plantwide control, throughput manipulator, MV-MV switching, CV-CV switching, controllers with different setpoints, split range control.

## 1. Introduction

Process down-time due to failures, extended operation at non-optimum points, long periods of switch-over from one mode of operation to another or prolonged operation with off-specification products are identified as causes for economic loss in a chemical plant (Stephanopoulos & Ng, 2000). The root cause for these problems is often that the normal control system is not able to handle certain

disturbances or failures, which makes it necessary to switch some control loops to manual mode.

In general, the operation of a system has two main objectives. The first is to stabilize the process and avoid that it drifts into an undesired operating region. The second is to minimize the economic cost $J$ (or equivalently maximize the profit) subject to satisfying the operational constraints. The focus in this paper is on the economic objective.

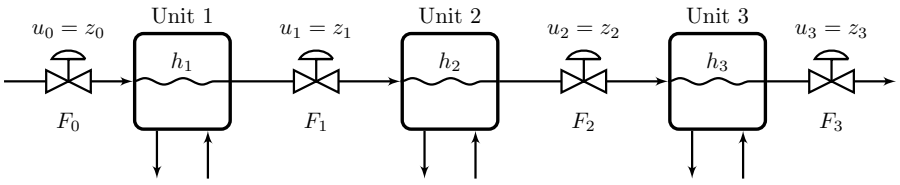


Figure 1: Flowsheet of the three units in series studied in this work. For simplicity the inventory is assumed to be liquid, but it could also be gas. We will not include the six flows without a valve in the later figures. These can be considered additional disturbances.

Fig. 1 shows a simplified process consisting of three units ($N = 3$) in series which we consider. In Fig. 1, there are four manipulated variables (MVs), which are the adjustable flows $F_k$ (valves $z_k$) into and out of each unit. Three of these MVs must be used to control (stabilize) the inventory (level) in the units, whereas the remaining degree of freedom, which we denote the throughput manipulator (TPM), sets the flowrate through the system. Although most process plants have some units in series, this is certainly not a general processing flowsheet, as for example, recycle flows are not included. Nevertheless, it is a fairly general structure for the case where we have $N$ inventories that should be controlled using $N + 1$ MVs. The inventories need to be controlled with given minimum and maximum bounds but otherwise the inventory (buffer) setpoints are degrees of freedom for optimizing the economics (minimizing operational cost $J$). This decision is a key part of the present paper.

The location of the TPM has a significant effect on the structure of the inventory loops which have to be radiating around the bottleneck for steady-state consistency (Price et al., 1994) (see also Fig. 3). The desired production rate is

typically set by the production planning team, and this determines the desired value (setpoint) for the TPM (at least when averaged over time). In other cases, the production rate may be set by one critical unit, which should operate at a fixed or maximum production rate (for example, the paper machine in a pulp and paper mill). However, during operation one may encounter disturbances which restrict the processing capacity. One important disturbance, which is the main focus in this paper, is a temporary or permanent reduction of the flow through one of the units, that is, the appearance of a new bottleneck in the process.

**Bottleneck definition.** *A bottleneck is an active constraint that limits further increase in throughput (gives maximum network flow subject to feasible operation).*

There may be some flexibility in temporarily isolating or containing a temporary bottleneck by making use of the stored or available (empty) buffer volume by temporarily giving up inventory control. However, inventories are restricted by minimum and maximum values, hence eventually it will be necessary to either stop production or to move the TPM to the new bottleneck, thus to rearrange the inventory loops correspondingly.

From this, we identify two challenges when encountering a new bottleneck:

**Challenge 1.** *Use of intermediate storage for bottleneck isolation (containment): How to optimally select the inventory (level) setpoints to maximize the time until a new bottleneck makes it is necessary to decrease the throughput?*

**Challenge 2.** *Inventory control rearrangement to handle bottlenecks: How to implement a logic that automatically rearranges the inventory loops to maintain consistent inventory control when encountering a new bottleneck?*

In this work, we explore these challenges by considering temporary and permanent bottlenecks. For a *temporary bottleneck*, the duration of the new active constraint may be short enough to isolate locally its effect such that we can utilize the buffer capacity thus avoid reducing the TPM (challenge 1). For a *permanent* bottleneck, the new active constraint propagates to the adjacent units and, after some delay which we want to maximize (challenge 1), we will

need to rearrange the loops and reduce the TPM (challenge 2).

Mathematically, let the MVs be the four valve positions in Fig. 1: $u = [z_0\ z_1\ z_2\ z_3]$, and let $\bar{F}$ denote the average production over a given time $T$

$$\bar{F} = \frac{1}{T}\int_0^T F_k(t)dt, \qquad k \in [0 \dots N]. \tag{1}$$

The primary operational objective is to keep $F_k$ at a given location $k$ at a given value (setpoint) $F_k^s$, but if this cannot be achieved, the average production should be maximized (Eq. 2a). Thus, the operational objective is to maximize $\bar{F}$ subject to Eq. 2b. The buffer inventories (levels $h_i$) in each tank they must be kept within high and low bounds (Eq. 2c). The degrees of freedom $u$ are the valve positions $z$. They are physically limited by upper and lower bounds (Eq. 2d), where typically $z^{\min} = 0$ (fully closed valve) and $z^{\max} = 1$ (fully open valve).

$$J = \max_u \bar{F} \tag{2a}$$

$$\text{s.t.} \quad F_k(t) \le F_k^s(t) \qquad \forall k \in [0, \dots, N] \tag{2b}$$

$$h_i^{\min} \le h_i(t) \le h_i^{\max} \qquad \forall i \in [1, \dots, N] \tag{2c}$$

$$z_k^{\min} \le z_k(t) \le z_k^{\max} \qquad \forall k \in [0, \dots, N] \tag{2d}$$

The main disturbances will be assumed to be changes in the maximum flow through the units, which may be represented as a change in $z_j^{\max}$.

These operational objectives are also found in batch-plant scheduling and the operation research literature under the names intermediate storage (Lee & Reklaitis, 1989) or buffer management strategy (Chong & Swartz, 2016). For example, the work by (Dubé, 2000) presents a numerical optimization method with the objective of maximizing throughput by coordinating the inventories for planned and unplanned shutdowns and reducing down time. This means that previous work benefits from pre-shutdown preparation, that is, charging the inventory of the tank downstream in anticipation of *a-priori* known reduced

production or shut-down upstream.

In this paper, we consider the use of standard advanced control, which includes the use of single-loop decentralized PID controllers combined with simple blocks such as selectors. The original goal of this work was to propose a simple control structure to automatically rearrange the inventory control loops (challenge 2). This corresponds to automatic MV-MV switching. The first obvious choice is to use split range control (SRC) (Reyes-Lúa & Skogestad, 2020b). However, SRC (for MV-MV switching) in combination with selectors (for CV-CV switching) is difficult to implement in a way that avoids delays during switching. An alternative to SRC is to use two controllers, one for each level setpoint (H and L). The resulting proposed control strategy is shown in Fig. 2. A similar control strcuture is presented in Shinskey (1981), ch. 3.7. The main difference is that we present a more detailed analysis of how it solves both challenges 1 and 2.

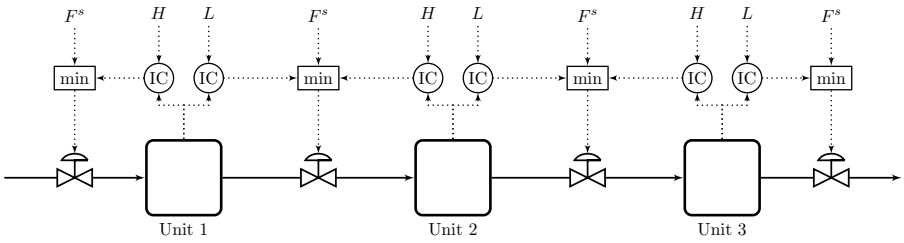


Figure 2: Bidirectional inventory control (IC) using selectors as proposed by (Shinskey, 1981). $H$ and $L$ are the high and low inventory setpoints. The operator can set the desired throughput $F^s$ at any given location ($k \in [0 \dots N]$). $F^s$ should be set to $F^s = \infty$ to maximize throughput at this location.

The structure of the paper is as follows. In Section 2, we consider conventional inventory control with a fixed structure, in Section 3 we answer challenge 1 and in Section 4 we address challenge 2. Serendipitously, as shown in Section 5, the structure in Fig. 2 chooses the level setpoints in an optimal manner and thus solves both challenges 1 and 2. In Section 6, we further discuss the TPM location and alternative implementation (e.g. model predictive control). In Section 7, we make our final conclusion.

## 2. Inventory (level) control with fixed control structure

In this section, we consider inventory control with a fixed control structure (fixed pairings), and review existing results. Level control is common in process plants and it has been extensively studied in the literature (Buckley, 1964; Marlin, 2000; Seborg et al., 2003; Shinskey, 1988; Stephanopoulos, 1984).

We consider the use of single-loop controllers. There are then two decisions that we need to make:

1. Choice of input-output pairings for inventory controllers.
2. Controller tuning.

We will consider them in opposite order.

### *2.1. Tuning of inventory controllers*

With a fixed level control pairing, there are two extreme cases which are frequently studied in the literature, *tight* and *averaging* level control (Marlin, 2000). The main difference between the two is in the selection of controllers tuning parameters.

**Tight level control.** The control objective is to keep the level ($y$) close to its setpoint ($y^s$), and MV variations are not important. In this case, we want to use *tight* tunings (largest possible controller gain subject to satisfying robustness requirements). For example, using the SIMC tuning rules (Skogestad, 2003), we select the closed loop time constant $\tau_C = \theta$, where $\theta$ is the effective time delay in the level loop.

**Averaging level control.** The objective is to average out the flow disturbances by allowing variations in the level. There is no fixed level setpoint except for keeping the level within bounds. Thus the control objective is to minimize the dynamic MV variations. This may be important if MV variations cause disturbances to other units. In this case, we want to use *smooth* tunings (smallest possible controller gain subject to satisfying level constraints).

For example, Skogestad (2006) recommends for *smooth* tunings to choose the minimum proportional gain $K_C$, and the integral time $\tau_I$ as given in Eq. 3.

$$K_C = \frac{|\Delta F|}{|\Delta h|} \tag{3a}$$

$$\tau_I = 4\tau_r \tag{3b}$$

where $|\Delta F|$ is the maximum change in flow disturbance,$|\Delta h|$ is the maximum allowed change in the level $h$, and $\tau_r$ is the tank residence time.

In this paper, we allow for level variations, so one may at first think that this is a use of *averaging level control* where smooth tunings are desired. However, the objective is not to minimize the dynamic MV variations, but rather to maximize the flow through the system subject to satisfying the level and flow constraints in Eq. 2c and Eq. 2d, respectively. The optimal is then to use tight level control tunings to be able to make full use of the buffer volume by operating close to the physical constraints $h^{\max}$ and $h^{\min}$. Note that the high (H) and low (L) inventory setpoints in Fig. 2 are set fairly close to these physical constraints.

### *2.2. Input-output pairings for consistent inventory control*

As we will see, for consistency the choice of input-output inventory pairings depends on the location of the throughput manipulator (TPM), so let us first define the TPM and consistency (Aske & Skogestad, 2009).

**Throughput manipulator (TPM).** *A TPM is a degree of freedom that affects the network flow, and which is not directly or indirectly determined by the control of the individual units, including their inventory control.*

For systems operating at maximum production, we have reached a bottleneck (active constraint) such that there is not really any degree of freedom left for changing the network flow. In such cases, we will refer to this limiting bottleneck (active constraint) as the TPM. This is in agreement with the above definition, because the limiting value of the active constraint affects the network flow.

**Consistency.** *An inventory control system is said to be consistent if the steady-state mass balances are satisfied for any part of the process, including the*

*individual units and the overall plant. Consistency is equivalent with internal stability of the system, and therefore this is a required property for steady-state operation. In addition, we usually want to have* local consistency*, which means that we want to control all inventories locally, that is, using the local inflow or outflow.*

For local consistent inventory control we need to follow the radiation rule, which says that the input-output pairings must be radiating around the location of a given flow (TPM) (Price et al., 1994).

**Radiating rule for local consistency.** *Inventory control must be in the direction of flow downstream the location of a given flow (TPM). Inventory control must be in the direction opposite to flow upstream the location of a given flow (TPM).*

For the simple example process in Fig. 1, the radiating rule leads to the four different pairing solutions in Fig. 3 (Price et al., 1994). The aim of this paper is to follow the radiating rule.

It is also possible to have consistent structures with use of non-local pairings ("long loops") that do not follow the radiating rule. One example is shown in Fig. 4 for the case with the TPM located at the feed $F_0$. It is possible to device more complex rules for the consistency of such complex structures (see for example Kida (2004), in Japanese) and one important rule is that it is not allowed to have any inventory loops crossing the TPM location. However, such complex structures with "long loops" are undesirable for obvious reasons and will not be considered in this paper.

## 3. Optimal inventory (buffer) setpoints (challenge 1)

In this section, we analyze how to isolate or contain the effect of bottlenecks for as long time as possible. We consider here the case of a temporary bottleneck. As an example, consider a temporary flow reduction (new bottleneck) in the feed $F_0$ for a case where $F_0$ is used for inventory control of a downstream unit (Fig. 3b, Fig. 3c and Fig. 3d). If we do nothing, then the level ($h_1$) in unit 1

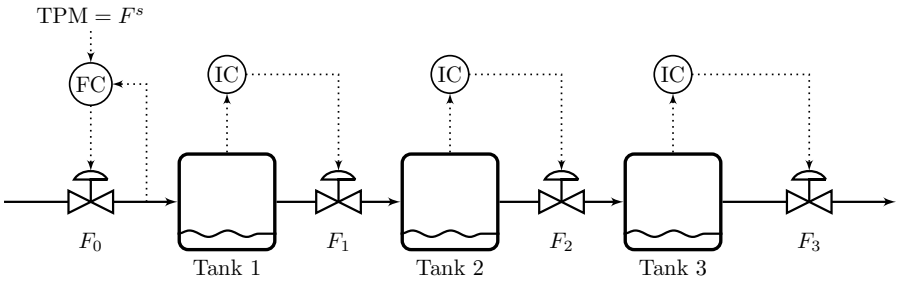


(a) The TPM location is at the plant feed at $F_0$. Inventory control in direction of flow.

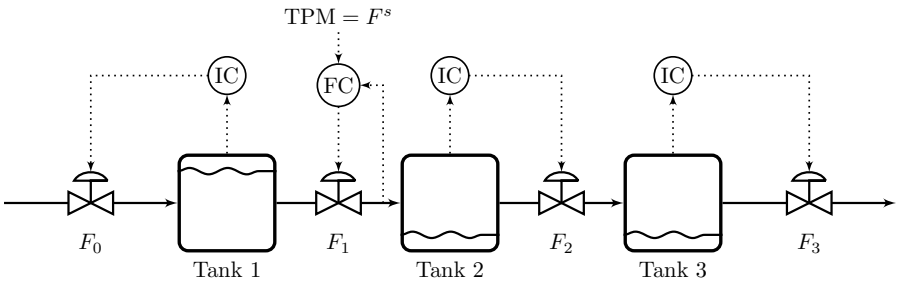


(b) The TPM location is inside the plant at $F_1$. Inventory control radiating around the TPM.

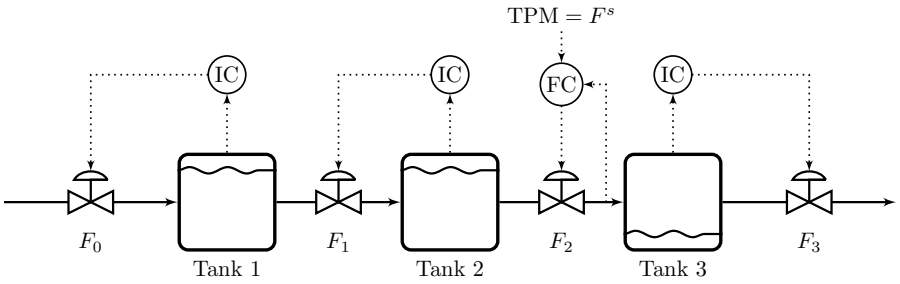


(c) The TPM location is inside the plant at $F_2$. Inventory control radiating around the TPM.

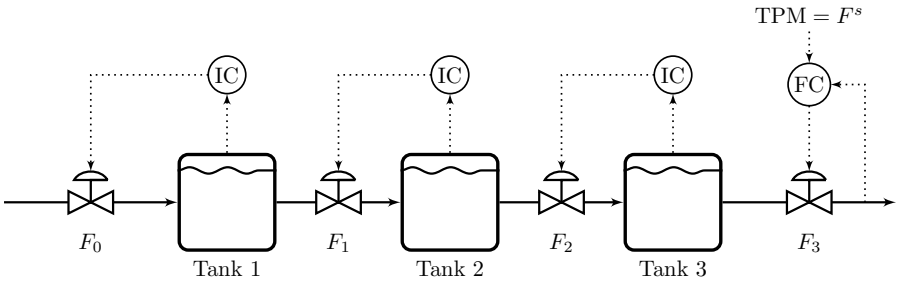


(d) The TPM location is at the plant product at $F_3$. Inventory control in direction opposite of flow.

Figure 3: Locally consistent inventory control system radiating around the throughput manipulator (TPM). The location of the TPM also determines the optimal inventory setpoints for temporarily isolating the effect of new bottlenecks on the TPM flowrate (see Section 3).

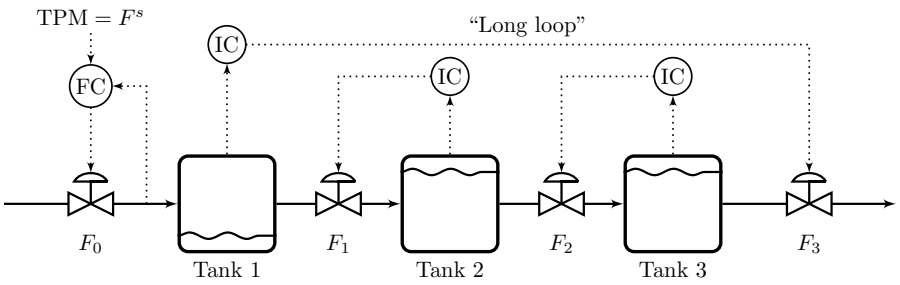


Figure 4: Consistent (but not locally consistent) inventory control structure with undesirable non-local pairing ("long loop"). Such structures are not studies in this paper.

starts falling below its setpoint ($h_1^s$) and without input constraints, $h_1$ reaches its minimum value $h_1^{\min} = 0\,\%$ after the buffer time

$$t_{b1} = \frac{A_1(h_1^s - h_1^{\min})}{\Delta F_0} \tag{4}$$

Here $\Delta F_0$ is the reduction in the flowrate $F_0$ and $A_1$ [$m^2$] is the unit (tank) cross-sectional area which we for simplicity have assumed is constant. We assume that $h_1^s = 0.9h_1^{\max} = 2.07\,\text{m}$ and $h_1^{\min} = 0\,\text{m}$. Setting $\Delta F_0 = 0.5F_0$ and substituting the model parameters given in Appendix A in Eq. 4 yields $t_{b1} = 4.14\,\text{min}$. This means that if the downtime for $F_0$ is less than $t_{b1}$, then the strategy of doing nothing will be acceptable, and give no loss in the production rate (reduction of the TPM). This is confirmed by a simulation of a flow reduction from 100% to 50% of its original value for 3 min in Fig. 5 (see Appendix A for model parameters and controllers tunings ). We see that we by making use of the stored volume in tank 1 have been able to isolate the effect of the temporary reduction in the flow $F_0$ to tank 1. From this simple analysis we conclude that in order to maximize the time $t_{b1}$, we should maximize the value of $h_1^s$, that is, to have a high inventory setpoint if the inventory is controlled by the inflow.

For similar reasons, it will be optimal to have low inventory setpoints if the outflow is used for inventory control. A simulation is shown in Fig. 6 for a 5 min temporary flow reduction (bottleneck) in $F_2$.

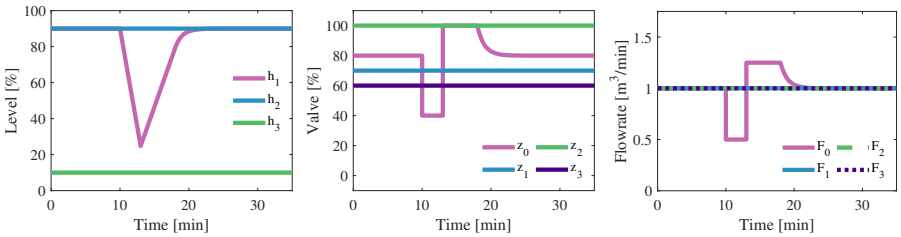


(a) Levels (CVs) (b) Valve positions (MVs) (c) Flows

Figure 5: Simulation of a 3 min temporary bottleneck in feed flow $F_0$ used for control of downstream level for the control structures in Fig. 3b, Fig. 3c and Fig. 3d. Note that the downstream flowrates ($F_1$, $F_2$ and $F_3$ are not affected.)

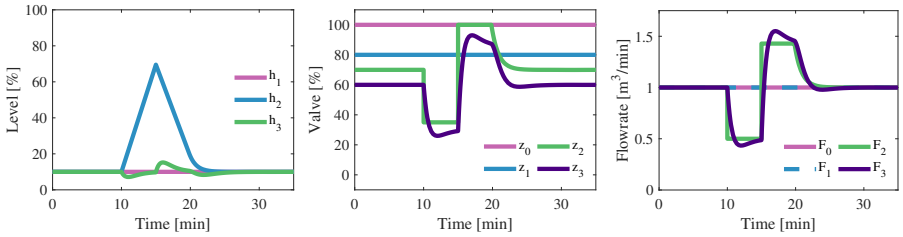


(a) Levels (CV) (b) Valve positions (MVs) (c) Flows

Figure 6: Simulation of a 5 min temporary bottleneck in flow $F_2$ used for control of upstream level $h_2$ for the control structures (Fig. 3a and Fig. 3b). Note that the upstream flowrates ($F_0$ and $F_1$ are not affected).

This leads to the following general rule for selection of inventory setpoints (which provides the solution to challenge 1).

**Rule for bottleneck isolation (Fig. 3).** *To delay as long as possible the time before a new bottleneck will affect other units, the inventory setpoints should be set high for all inventories controlled by the inflow and the inventory setpoint should be set low for all inventories controlled by the outflow.*

A closer look at Fig. 3 shows that all the inventories have been selected to follow this rule. Also note that Fig. 4 follows this rule.

## 4. Inventory control rearrangement to handle bottlenecks (challenge 2)

Let us first note that the TPM sets the steady-state flow through the system. If we during a dynamic transition fix also another flow or encounter a new bottleneck, then there will temporarily be two TPMs and this inconsistency is resolved by temporarily giving up the control of one of the inventories. This was what we did in Section 3 (Fig. 5 and Fig. 6), but the bottleneck was temporary so it was not necessary to move the TPM and rearrange the inventory control loops. We now expand the analysis to a longer time or even permanent bottleneck. The goal is therefore to identify the new bottleneck, and select it as the new TPM and then rearrange the inventory loops between the new and old TPM such that we follow the radiation rule (Fig. 3). For example, if originally the TPM is at the product $F_3$ (Fig. 3d), but then the feed rate $F_0$ becomes the bottleneck, we would need to rearrange all the three level loops to get the structure in Fig. 3a. It may seem that this requires a centralized supervisor which identifies the new bottleneck and then uses logic to rearrange the control loops accordingly. However, as shown in this section, it can be achieved also with decentralized single-loop PID controllers (Fig. 2).

The root cause for rearranging loops is that we have encountered a new bottleneck. That is, a manipulated variable (MV) used for level control is saturated and no longer available. However, we want to maintain level control

and therefore need to find a *new* MV to use. This is the issue of MV-MV switching. However, since all MVs are already used to control other CVs, we need in addition a CV-CV switching, that is, a min or max selector (Reyes-Lúa & Skogestad, 2020b).

### *4.1. MV-MV switching*

For MV-MV switching (bidirectional inventory control), we will consider two alternatives (Reyes-Lúa & Skogestad, 2020b)

1. split range control
2. two controllers, with different inventory setpoint (high and low)

### *4.2. CV-CV switching: selectors*

Selectors logic blocks, also called overrides, are used when only one MV is available for several CVs. The solution is to use an independent controller for each CV and a min or max selector (or combination) to select the plant input ($u$) from all controller outputs ($u_i$). Fig. 7 shows the block diagram for two CVs and one MV.

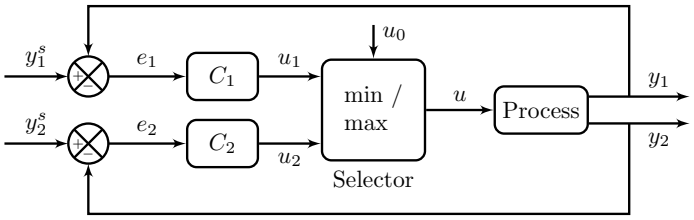


Figure 7: Selector (min or max) to switch from controlling CV1= $y_1$ to CV2= $y_2$ when CV2 becomes an active constraint.

The work by (Krishnamoorthy & Skogestad, 2020) presents a systematic design procedure for selectors. The theory states that a max-selector is used for constraints that are satisfied with a large input, and a min-selector for constraints that are satisfied with a small input.

*4.3. Bidirectional inventory control using SRC and* min − *selectors*

Fig. 8 shows the bidirectional inventory control structure using SRC for MV-MV switching and min-selectors for CV-CV switching. In Fig. 8, $z_k^1$ sets the desired flow at location $k$ (it is set at $\infty$ if the goal is to maximize at this location), and the remaining signals $z_k^i$ are the SRC outputs from the inventory controllers.

However, SRC is not recommended in combination with CV-CV switching because of delays in switching as it is also apparent from the simulation in Fig. 9 and also discussed in Appendix E. The responses in Fig. 9 are for a permanent reduction of 50 % at the plant feed ($F_0$) which implies reconfiguring the inventory loops to move the TPM from the product ($F_3$) to the feed ($F_0$). The SRC scheme is able to handle the reconfiguration of loops, but as it can be seen from Fig. 9, the level control is not very good and there are large overshoots in the MVs (flows). The reason is that SRC in combination with CV-CV switching results in delays in the MV-MV switching. The reason for the delay is that the min and max limits in the split range block are not the same as the actual values encountered during switching (see Appendix E). There are possible ways to avoid this, but it becomes complicated to implement (see Appendix E.1). Fortunately, there is a simpler alternative solution, namely to use controllers with different setpoints (Fig. 10).

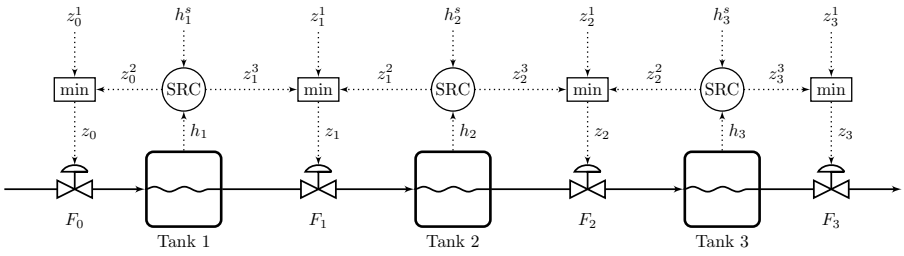


Figure 8: Bidirectional inventory control with SRC for MV-MV switching and min-selectors for CV-CV switching. The scheme rearranges the inventory control loops (challenge 2) but it does not solve challenge 1 of optimizing the inventory setpoints because $h_i^s$ is fixed.

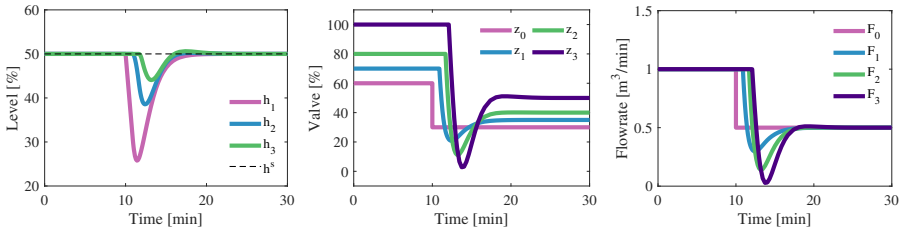


(a) Levels (CVs) (b) Valve positions (MVs) (c) Flows

Figure 9: Simulation of the SRC structure (Fig. 8) for reconfiguring the inventory loops to move the TPM from $F_3$ to $F_0$. The plant feed $F_0$ decreases by 50 % at time $t = 10$min.

### *4.4. Bidirectional inventory control using controllers with different setpoints and* min *selectors*

Fig. 10 shows the bidirectional inventory control structure using two controllers, with different setpoints (H and L), and min-selectors. In Fig. 10, $z_k^1$ sets the desired flow at location $k$, $z_k^2$ is the output of the controller with a high (H) inventory setpoint located downstream of valve $k$ for $k = [0, 1, 2]$, and $z_k^3$ is the output of the controller with a low (L) inventory setpoint located upstream of valve $k$ for $k = [1, 2, 3]$.

Since the root cause is that we have encountered a new bottleneck, it means that we must reduce the flow. Thus, a min selector is needed. From this the proposed structure in Fig. 2 (and in Fig. 10) follows directly. The main difference between Fig. 2 and Fig. 10 is that we in Fig. 2 have implicitly assumed to have implemented flow controllers (although not shown), whereas we in Fig. 10, directly manipulate the valve positions $z_k$. Otherwise, they behave in the same way, and they will always maximize the network flow and keep the levels within bounds. We can set the flow at any location $k$ by setting $F^s$ in Fig. 2 or $z_k^1$ in Fig. 10, but it will only be selected if it is sufficiently low such that it becomes a bottleneck for the network.

Fig. 11 shows the simulation responses for a permanent reduction of 50 % at the plant feed ($F_0$) which implies reconfiguring the inventory loops to move the TPM from the product ($F_3$) to the feed ($F_0$). To reduce the switching time and make the results more comparable to the SRC structure in Fig. 9, we use

a small difference between the high ($H$) and the low ($L$) setpoints (see Eq. 4); the high setpoint is $h_i^H = 55\,\%$ and the low setpoint is $h_i^L = 45\,\%$.

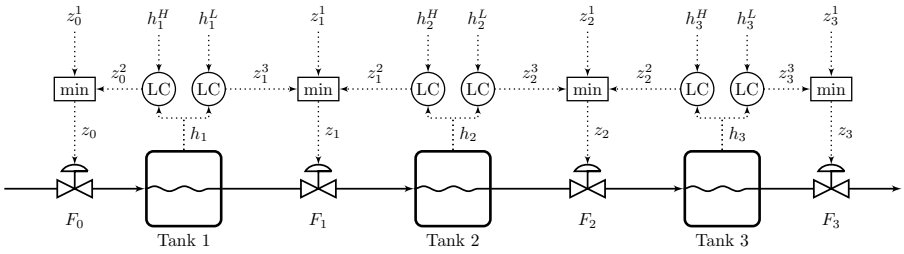


Figure 10: Proposed bidirectional inventory control structure, which lets the levels optimally vary between high ($H$) and low $L$ limits. This is the same structure as in Fig. 2, except that that we have introduced the valve position $z_i$ as the MV$_i$. This also allows for using valve saturation to represent new bottlenecks in the simulation.

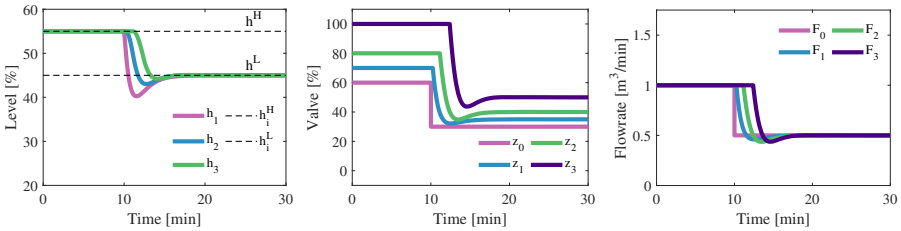


(a) Levels (CVs) (b) Valves positions (MVs) (c) Flows

Figure 11: Simulation of the proposed structure with different setpoints (Fig. 10) for reconfiguring the inventory loops to move the TPM from $F_3$ to $F_0$. Note that the difference between the level setpoints ($h_i^H = 55\%$ and $h_i^L = 45\%$) is quite small in this case to give a short switching time.

### *4.5. Comparison of the two bidirectional control structures*

The details of the tuning for the two bidirectional control (Fig. 8 and Fig. 10) structures are given in Appendix C and Appendix D, respectively. All controllers are PI-controllers tuned with the SIMC-rules (Skogestad, 2003) with the closed loop time constant $\tau_C = 0.5$ min, which gives an integral time $\tau_I = 4\tau_C = 2$ min.

The simulations show that the control structure with different setpoints (Fig. 10) is much better than with SRC (Fig. 8). As mentioned, the reason for the poor performance is the switching delays encountered within SRC. The

structure with different setpoints in Fig. 10 avoids these delays because the switching is done based on the CV measurement and not on the saturation limits of the MV as in SRC, and because of the use of antiwindup which tracks the plant input (we use a back-calculation implementation (Åström & Hägglund, 2006)). There will be some delay because of the difference in setpoints (H and L), but as shown next this can be an advantage.

In summary, we find that the scheme with two controllers (Fig. 10) is better for rearranging the inventory loops than standard SRC (Fig. 8). It is thus best for addressing challenge 2. Since it has two inventory setpoints it may also address challenge 1. This is discussed in the next section.

## 5. Optimal use of intermediate storage (challenges 1 and 2)

We have shown that the scheme in Fig. 2 and Fig. 10 with two controllers addresses challenge 2, and by making use of the two inventory setpoints (H and L) it can also optimally solve challenge 1. The reason is that the ordering of the level setpoints needed to address challenge 2 is consistent with the optimal setpoints given by the rule for bottleneck isolation given in section 3. That is, to make use of the maximum flexibility we select the setpoint $h^H$ close to $h^{\max}$ and the setpoint $h^L$ close to $h^{\min}$.

To better demonstrate the usefulness of this scheme, we show several simulation cases. We consider the case where the TPM is originally located at the product $F_3$, but the scheme works equally well with the TPM at other locations. Thus, originally, the controllers in Fig. 10 are active in the direction opposite of flow as shown in Fig. 3d, and with all levels at their high setpoints. The system is then ideally suited to delay the effect of bottlenecks appearing in the upstream process ($F_0$, $F_1$, $F_2$).

In Fig. 12, we consider a temporary (19 min) 50 % decrease in feed $F_0$, by changing $z_0^{\max}$ from 1 to 0.3. Because $F_0$ is located further away from $F_3$, we can make use of all the inventories $h_1$, $h_2$ and $h_3$ to isolate the effect of the new bottleneck in $F_0$ on $F_3$. This is the same case as in Fig. 11, but we have chosen

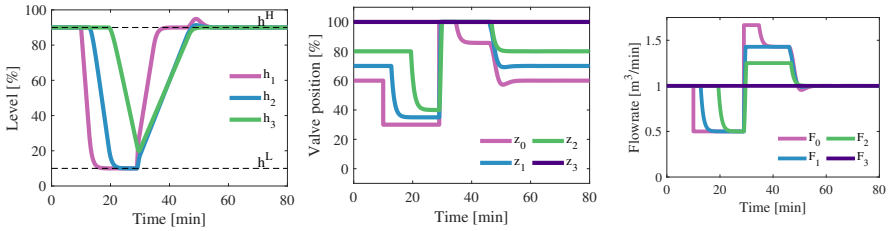


(a) Levels (b) Valve positions (c) Flows

Figure 12: Simulation of a temporary (19 min) 50 % decrease in feed $F_0$ for the proposed control structure in Fig. 10 at $t = 10$ min. The TPM is initially at the product ($F_3$). During the recovery period after $t = 29$ min, the flows are at their maximum value due to physical valve constraints.

the level setpoints far away ($h^H = 90\,\%$ and $h^L = 10\,\%$) in order to delay as much as possible the effect of the reduction in the feed $F_0$ on the product $F_3$. Initially, the system responds with the level $h_1$ dropping (Fig. 5a). When the level $h_1$ starts approaching its minimum value ($h_1^L$), the level controller with a low setpoint for $h_1$ becomes active and starts reducing $F_1$. This makes level $h_2$ drop and eventually this gives a reduction also in $F_2$. This effect propagates and $h_3$ starts decreasing. However, in this case the bottleneck in $F_0$ disappears at $t = 29$ min, before $h_3$ reaches its minimum value ($h_3^L$), and thus there is no effect on $F_3$. During the recovery period, when we want to increase $F_0$ again (and also $F_1$ and $F_2$), the flows $F_0$, $F_1$ and $F_2$ need to overshoot to regain the lost production, while $F_3$ is kept at its original desired throughput. Because the selector blocks have been set up to maximize the flow (we can show this more clearly by noting that we could have set $F_k^s = \infty$ or $z_k^1 = \infty$), we initially reach the maximum constraints on $F_0$, $F_1$ and $F_2$ (or more exactly on their valve positions). During the recovery period, we lose control of all inventories until they are close to their maximum bounds when the level controllers with high inventory setpoints ($h_i^H$) becomes active. Then, for $t > 60$ min (approximately), the inventory loops are again in the direction shown in Fig. 3d, and the system is prepared for future bottlenecks. Detailed response of the controller outputs are shown in Appendix B.

In Fig. 13, we consider a temporary (19 min) bottleneck (disturbance) for

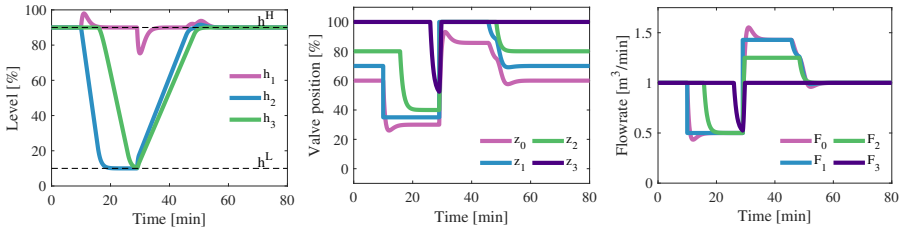


(a) Levels (b) Valve positions (c) Flows

Figure 13: Simulation of a temporary (19 min) bottleneck in flow $F_1$ for the proposed control structure in Fig. 10. The TPM is initially at the product ($F_3$).

$F_1$. Here the upstream level $h_1$ initially has a small increase above its high setpoint $h_1^H$, but it is restored to $h_1^H$ by the activation of the level controller which reduces $F_0$. In this case, the new bottleneck is closer to the TPM, so we have less isolation and we get a short-term reduction in the TPM $F_3$ at about $t = 28$ min.

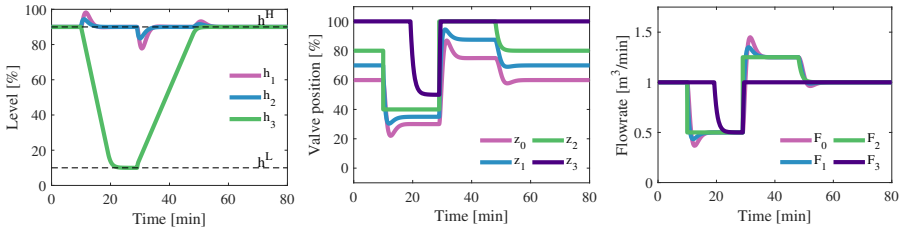


(a) Levels (b) Valve positions (c) Flows

Figure 14: Simulation of a (19 min) temporary bottleneck in flow $F_2$ for the proposed control structure in Fig. 10. The TPM is initially at the product $F_3$.

Finally, in Fig. 14, we consider a temporary (19 min) bottleneck for $F_2$. In this case, the new bottleneck is even closer to the TPM, and we get a reduction in the desired product (TPM) $F_3$ from $t = 20$ min. Note that we initially have some small increase on the levels $h_1$ and $h_2$. This makes the disturbance in $F_2$ propagate quickly to reduce $F_1$ and $F_0$.

Other simulations results are available in the master thesis by Lillevold Skaug (2020). These include the case with the TPM at the feed $F_0$, SRC with bias update, generalized SRC (extension to SRC that can handle different integral times (Reyes-Lúa & Skogestad, 2020a)), and model predictive control (MPC)

for tight inventory control.

## 6. Discussion

### *6.1. Choice of TPM location*

The proposed control system in Fig. 2 (and the more detailed Fig. 10) automatically moves the TPM to the new (permanent) bottleneck and reconfigures the inventory loops to give the arrangement in Fig. 3 (challenge 2). However, there may also be cases where the production rate is not determined by a bottleneck, but rather has a given setpoint, for example, determined by market conditions. Where should the TPM be located in this case? There may be many considerations. If we do not expect bottlenecks, then it is often recommended to locate the TPM at a place where we want small dynamic variations, for example, at the feed of a critical unit. For a process with a long recycle loop, it is often recommended to locate the TPM inside the recycle loop (Luyben, 1993). For cases where bottlenecks are expected, it is recommended in the literature that the TPM should be located at the expected future bottleneck (Aske et al., 2008). The reason is to be able to achieve tight control at the bottleneck when it occurs. This avoids "long loops" (Fig. 4) and reduces the back-off. However, this recommendation is under the assumption that we are not allowed to rearrange the inventory control loops, hence it does not apply for the proposal in Fig. 2 (and Fig. 10) with bidirectional inventory control . Interestingly, for the proposed control system in Fig. 2 (and Fig. 10), which have *automatic* reconfiguration of the loops, the recommendation is opposite: *The set flow $F^s$ (and thus the TPM) should be located as far away as possible from the expected next bottleneck.* We can then use all the inventories between the new bottleneck and TPM to isolate the new bottleneck, that is, we can delay as long as possible the time before we must reduce the throughput (challenge 1). Of course, if the bottleneck is permanent, the TPM will move to the new bottleneck, which is consistent with the recommendation by Aske et al. (2008).

### *6.2. Alternative implementation: model predictive control (MPC)*

MPC handles constraints changes by design, and it therefore seems to be a good alternative for our case. However, while it may be suited for fast MV-MV switching and tight level control (challenge 2), we do not see an easy implementation of changing the inventory setpoints in an optimal manner (challenge 1). A possible approach would be to predict some different scenarios, but this would be too complicated and it is not obvious how it could be implemented. Alternatively, logic could be used, but this required a separate supervisor in addition to MPC.

Moreover, the decentralized solutions that we propose in this work have six advantages over more advanced multivariable control such as MPC:

1. easier to implement
2. does not require a full dynamic plant model
3. require only local information (i.e. level measurement in our case)
4. do not require solving a dynamic optimization problems
5. do not require disturbance measurement or forecast
6. it is easier to embed information about what to do in case of future disturbances.

## 7. Conclusion

In this work we propose to use the bidirectional inventory control structure in Fig. 2 with a high and a low setpoints for each inventory. This scheme maximizes throughput when there are changes in the operation that give new temporary or permanent bottlenecks in other units. In order to isolate the effect of a new bottleneck, the inventories will be floating between the minimum and maximum values at certain times. This structure automatically identifies the new bottleneck without the need for centralized logic, and thus it automatically reconfigures the inventory loops to be radiating around the TPM to

get local consistency of the inventory control system (challenge 2). That is, it automatically gives the four desired structures in Fig. 3 as special cases. Moreover, it automatically adjusts the inventory setpoints for optimal disturbance isolation (challenge 1), by setting large inventory setpoint upstream TPM and small inventory setpoint downstream. Finally, it automatically recovers the lost production for a temporary bottleneck.

**Acknowledgements**

This work is partly funded by HighEFF Centre for an Energy Efficient and Competitive Industry for the Future. The authors gratefully acknowledge the financial support from the Research Council of Norway and user partners of HighEFF, an 8 year Research Centre under the FME-scheme (Centre for Environment-friendly Energy Research, 257632/20).

**References**

Aske, E. M. B., & Skogestad, S. (2009). Dynamic Degrees of Freedom for Tighter Bo ttleneck Co ntrol. In *10th International Symposium on Process Systems Engineering - PSE2009* (pp. 1275–1280). Elsevier Inc. volume 27. doi:10.1016/S1570-7946(09)70603-0.

Aske, E. M. B., Strand, S., & Skogestad, S. (2008). Coordinator MPC for maximizing plant throughput. *Computers and Chemical Engineering*, *32*, 195–204. doi:10.1016/j.compchemeng.2007.05.012.

Åström, K. J., & Hägglund, T. (2006). *Advanced PID-control*. ISA – Instrumentation, Systems, and Automation Society.

Buckley, P. S. (1964). *Techniques of Process Control*. (1st ed.). Delaware, USA: John Wiley and Sons.

Chong, Z., & Swartz, C. L. E. (2016). Optimal response under partial plant shutdown with discontinuous dynamic models. *Computers and Chemical Engi-*

*neering*, *86*, 120–135. URL: http://dx.doi.org/10.1016/j.compchemeng.2015.12.011. doi:10.1016/j.compchemeng.2015.12.011.

Dubé, J.-F. H. (2000). *Pulp mill scheduling: optimal use of storage volumes to maximize production*. Master of engineering McMaster University.

Kida, F. (2004). -. *Chem. Eng (Tokyo) (in Japanese)*, *49*, 144–151.

Krishnamoorthy, D., & Skogestad, S. (2020). Systematic design of active constraint switching using selectors. *Computers and Chemical Engineering*, *143*, 107106. doi:10.1016/j.compchemeng.2020.107106.

Lee, E. S., & Reklaitis, G. V. (1989). Intermediate storage and operation of periodic processes under equipment failure. *Computers and Chemical Engineering Chemical Engineering*, *13*, 1235–1243.

Lillevold Skaug, D. A. (2020). *Control structure for consistent inventory control with moving bottleneck*. Master thesis Norwegian University of Science and Technology. URL: folk.ntnu.no/skoge/diplom/diplom20/alexander-skaug/.

Luyben, W. L. (1993). Dynamics and control of recycle systems. 2. Comparison of alternative process designs. *Industrial and Engineering Chemistry Research*, *32*, 476–486. doi:10.1021/ie00015a011.

Marlin, T. E. (2000). *Process Control. Designing Processes and Control Systems for Dynamic Performance*. McGraw Hill.

Price, R. M., Lyman, P. R., & Georgakis, C. (1994). Throughput manipulation in plantwide control structures. *Industrial and Engineering Chemistry Research*, *33*, 1197–1207. doi:10.1021/ie00029a016.

Reyes-Lúa, A., & Skogestad, S. (2020a). Multi-input single-output control for extending the operating range : Generalized split range control using the baton strategy. *Journal of Process Control*, *91*, 1–11. doi:10.1016/j.jprocont.2020.05.001.

Reyes-Lúa, A., & Skogestad, S. (2020b). Systematic Design of Active Constraint Switching Using Classical Advanced Control Structures. *Ind. Eng. Chem. Res.*, *59*, 2229–2241. doi:10.1021/acs.iecr.9b04511.

Reyes-Lúa, A., Zotică, C., & Skogestad, S. (2019). Systematic Design of Split Range Controllers. *IFAC-PapersOnLine*, *53*, 898–903. doi:10.1016/j.ifacol.2019.06.176.

Seborg, D. E., Edgar, T. F., & Mellichamp, D. A. (2003). *Process Dynamics and Control*. (2nd ed.). John Wiley and Sons.

Shinskey, F. G. (1981). *Controlling multivariable processes*. Instrument Society of America.

Shinskey, F. G. (1988). *Process Control Systems.*. (3rd ed.). McGraw-Hill.

Skogestad, S. (2003). Simple analytic rules for model reduction and PID controller tuning. *Journal of Process Control*, *13*, 291–309. doi:doi:10.1016/S0959-1524(02)00062-8.

Skogestad, S. (2006). Tuning for Smooth PID Control with Acceptable Disturbance Rejection. *Ind. Eng. Chem. Res.*, *45*, 7817–7822. doi:10.1021/ie0602815.

Stephanopoulos, G. (1984). *Chemical Process Control: An Introduction to Theory and Practice*. Prentice-Hall.

Stephanopoulos, G., & Ng, C. (2000). Perspectives on the synthesis of plant-wide control structures. *Journal of Process Control*, *10*, 97–111.

## Appendix A. Process model and parameters

Assuming constant density ($\rho$) and constant cross-sectional tank area, the mass balance for each tank is

$$\frac{dh_i}{dt} = \frac{1}{A_i}(F_{i-1} - F_i) \quad \forall \imath \in (1, 2, 3) \tag{A.1}$$

where $h\,[\mathrm{m}]$ is the level, $A\,[\mathrm{m}^2]$ is the cross-sectional tank area (Table A.1) and $F\,[\mathrm{m}^3\,\mathrm{min}^{-1}]$ is the volumetric flowrate in and out of the tank respectively calculated from Eq. A.2.

$$F_i = \underbrace{C_{v,i}\sqrt{\frac{\Delta P_i}{\rho}}}_{k_{v,i}} f_i(z) \quad \forall_1 \in [0,1,2,3] \tag{A.2}$$

where $C_v$ is the valve coefficient, $\Delta P\,[\mathrm{Pa}]$ is the pressure drop over the valve assumed constant, $\rho\,[\mathrm{kg}\,\mathrm{m}^{-3}]$ is the water density assumed constant and $f(z)$ is the valve characteristic, which we assume linear, i.e. $f(z) = z$,.

Table A.1 shows the tank design parameters, $V_{\mathrm{Tank}}$ is the design volume, $A$ is the tank cross-sectional areaand $h_{\mathrm{Tank}}$ is the tank design height.

Table A.1: Design parameters for the three tanks

| $i$ | $V_{\mathrm{Tank}}\,[\mathrm{m}^3]$ | $A\,[\mathrm{m}^2]$ | $h_{\mathrm{Tank}}\,[\mathrm{m}]$ |
|---|---|---|---|
| 1 | 2.3 | 1 | 2.3 |
| 2 | 4.2 | 1.5 | 2.8 |
| 3 | 6.4 | 2 | 3.2 |

Table A.2 shows parameter $k_v$ (Eq. A.2) for the four valves together with the nominal valve openings ($z^*$) corresponding to a flow value of $F = 1\ \mathrm{m}^3\,\mathrm{min}^{-1}$. Note that for the different cases we locate the smallest $k_v$ value at the original TPM at $z^{\max} = 1$, and this is the reason for the different initial valve openings between Fig. 6, Fig. 5 and Fig. 12.

Table A.2: Design parameters for the four valves.

| $z^*$ | $k_v\,[\mathrm{m}^3\,\mathrm{min}^{-1}]$ |
|---|---|
| 1 | 1 |
| 0.8 | 1.25 |
| 0.7 | 1.428 |
| 0.6 | 1.667 |

## Appendix B. Controllers outputs for the structure in Fig. 10

Fig. B.15 complements the simulation results in Fig. 12 and it shows the inputs to (interrupted lines), and the outputs from (continuous lines) the four min selectors blocks of the structures with controllers with different setpoints (Fig. 10).

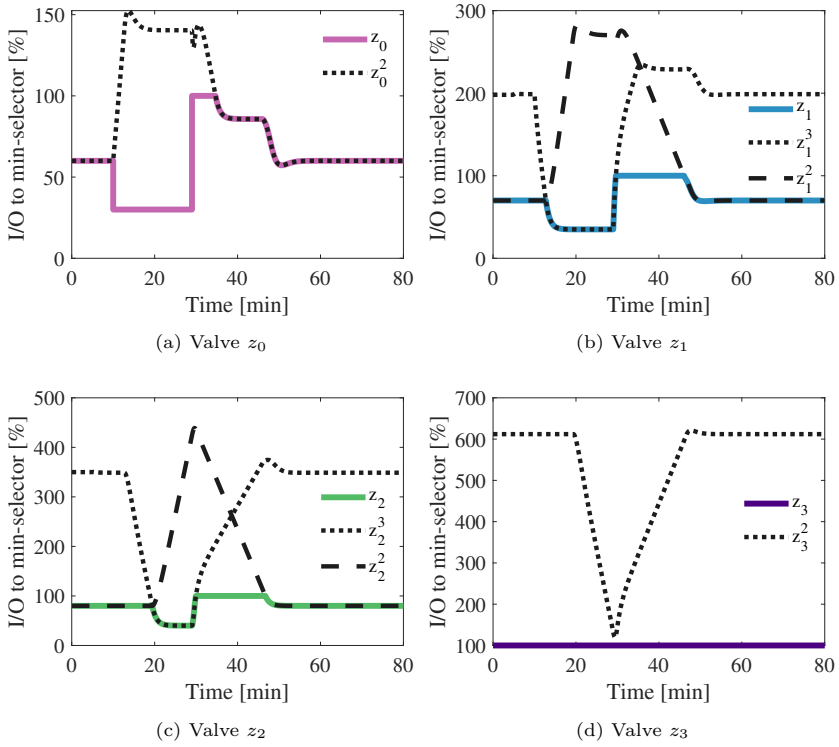


(a) Valve $z_0$ (b) Valve $z_1$

(c) Valve $z_2$ (d) Valve $z_3$

Figure B.15: Inputs and outputs for all min −selectors in Fig. 10 corresponding with the simulation responses in Fig. 12. The continuous line is the selected physical valve position. To maximize throughput we set $z_0^1 = z_1^1 = z_2^1 = z_3^1 = \infty$.

## Appendix C. Tuning of controllers with different setpoint

We can tune the two PI-controllers independently, meaning that we can consider the different effects from the MVs (valves) on the CV (level) given by the different valve characteristics $C_v$ and and pressure drops ($\Delta P$) over the

Table C.3: Tuning parameters for controllers with different setpoints.

| Tank | LC | $h^s$ | $K_C$ TPM=$F_0$ | $K_C$ TPM=$F_2$ | $K_C$ TPM=$F_3$ | $\tau_I$ [min] | $\tau_T$ [min] | $\tau_C$ [min] |
|---|---|---|---|---|---|---|---|---|
| 1 | high | 90 % | 2 | 1.6 | 1.2 | 2 | 1 | 0.5 |
| | low | 10 % | -1.6 | -1.4 | -1.4 | 2 | 1 | 0.5 |
| 2 | high | 90 % | 2.4 | 2.1 | 2.1 | 2 | 1 | 0.5 |
| | low | 10 % | -2.1 | -3 | -2.4 | 2 | 1 | 0.5 |
| 3 | high | 90 % | 2.8 | 4 | 3.2 | 2 | 1 | 0.5 |
| | low | 10 % | 2.4 | -2.4 | -4 | 2 | 1 | 0.5 |

valve. For example, we may apply the SIMC tuning rules (Skogestad, 2003) to the model given in Appendix A, which is an integrating process with a large open loop time constant $\tau \to \infty$. Table C.3 shows the tuning parameters. These are the high and low level setpoints ($h^s$), the controller proportional gain $K_C$, the integral time $\tau_I$, and the tracking time constant $\tau_T$. Here, $\tau_C$ is the desired closed loop time constant.

## Appendix D. Tuning of SRC

We follow the procedure proposed by Reyes-Lúa et al. (2019) to tune the SRC parameters. These are the common controller gain $K_C$, the common integral time $\tau_I$ and the individual slopes $\alpha_i$. The slopes $\alpha_i$ allow for different controller gains for each MV considering the different valve size (Eq. D.1a). We define the normal range for the internal signal $v$ to be from 0 % to 100 %, and we scale the MVs also from 0 % to 100 %. Then, for each tank, we solve the system formed by the Eq. D.1.

$$K_{C,i} = \alpha_i K_C, \quad \forall i \in (1,2) \tag{D.1a}$$

$$\Delta v_1 + \Delta v_2 = 100 \tag{D.1b}$$

$$\Delta v_i = \frac{u^{\max} - u^{\min}}{|\alpha_i|} = \frac{100}{|\alpha_i|}, \quad \forall i \in (1,2) \tag{D.1c}$$

where the significances of $\Delta v$ and $\alpha$ are shown in Fig. D.16a.

However, we can only have one integral time ($\tau_I$) and we need to compromise

Table D.4: Modified $K_C$ and $\tau_I$ for the three SRC in Fig. 8.

| Tank | $h^s$ | $K_C$ | $\tau_I$ | $\tau_C$ min | $\alpha_1$ | $\alpha_2$ | $v^*$ | $u_{0,1}$ | $u_{0,2}$ |
|---|---|---|---|---|---|---|---|---|---|
| 1 | 50 % | 65 | 2 | 0.5 | 1.8571 | -2.1667 | 53.85 | 0 | 216.167 |
| 2 | 50 % | 112 | 2 | 0.5 | 1.875 | -2.1429 | 53.33 | 0 | 214.286 |
| 3 | 50 % | 178 | 2 | 0.5 | 1.8 | -2.25 | 55.55 | 0 | 225 |

on its value. Because the slowest process is critical we select the largest $\tau_I$ of the two options (for inlet and outlet valves in Table C.3). However, with no delay and same $\tau_C$, all $\tau_I$ are equal. However, the common controller gains $K_C$ were found to be too small in simulations, and the min selector output would alternate between the two controllers. To improve the dynamic performance, we increased them and the new values are given in Table D.4. The slopes $\alpha$ remain the same.

Fig. D.16a shows the split range block for tank 1. Fig. D.16b shows the split range block for tank 2. Fig. D.16c shows the split range block for tank 3.

## Appendix E. Performance of bidirectional inventory control using SRC

SRC gives poor level control, especially of $h_1$ (Fig. 9a). The reason is that there are two delays in the MV-MV switching. Initially, the TPM is a the product $F_3$ (Fig. 3d), and the valve openings are $z_0 = z_0^2 = 0.6$ and $z_1 = z_1^2 = 0.7$ (Fig. 8). Then at $t = 10$ min, the feed flow $F_0$ drops to 50 % of its original value. In the simulation, we do this by changing the value of $z_0^1$ from 1 to 0.3, but physically it could be caused by a bottleneck inside process which the controller does not know about. This causes the level $h_1$ in tank 1 to drop, and the SRC responds by trying to open the valve $z_0$. This has no initial effect because $z_0$ is fixed at $z_0 = 0.3$ due to the bottleneck in the unit. This causes the first delay. Eventually, when $z_0$ reaches 1 (the max-value in the SR-bock), the SRC switches the MV to $z_1$, which starts at its max value, $z_1^3 = 1$, which is larger then the nominal $z_1^2 = 0.7$. Thus, the action of SRC now has to decrease the value down to $z_1 = 0.7$ before the min-selector changes the level control

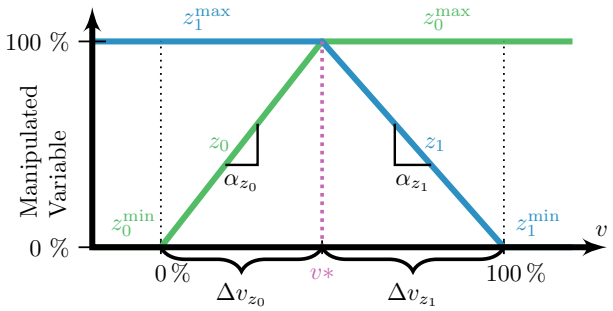


(a) Tank 1

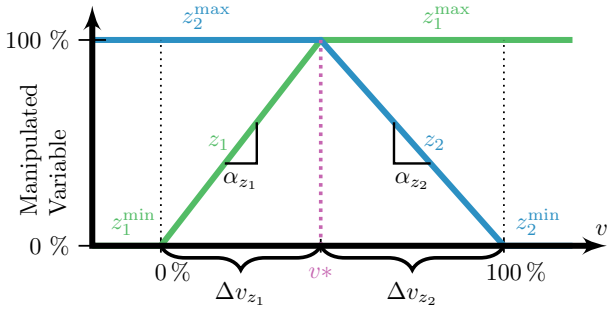


(b) Tank 2

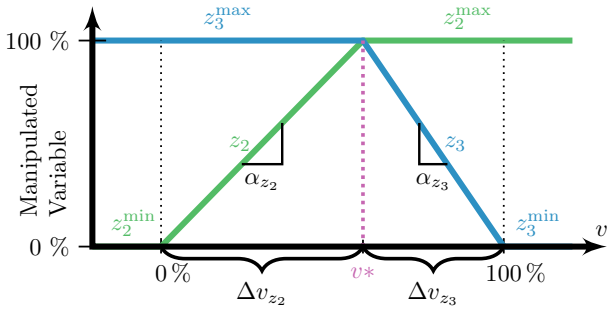


(c) Tank 3

Figure D.16: Split range blocks for Fig. 8.

direction. This causes the second delay, before finally the action of SRC has some effect on the level $h_1$. To improve the level control performance for SRC, we may do some more complex fixes such as updating the bias for the internal controller.

*Appendix E.1. Bias update for SRC*

We propose here a method to avoid the two delays in switching within SRC and achieve tight level control by updating the bias for the internal controller. In Fig. E.17, we make a "jump" in $\Delta v$ such that the switching happens immediately, without having to wait for the signal $v$ to travel the pattern area. The figure refers to tank 2 in particular, but it is also valid for the other two tanks.

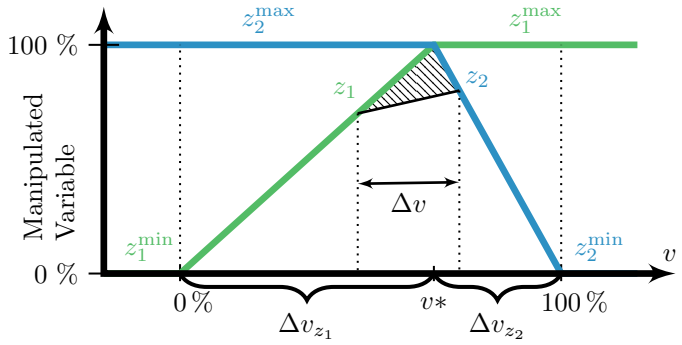


Figure E.17: Possible bias update for SRC for tank 2 to achieve tight level control. Without the update, the controller would have to integrate over the pattern area which is the cause of the delay in switching.

To compute what the actual value of $z_2$ should be, we set $F_1 = F_2$, and invert the valve equation (Eq. A.2) to solve for $z_2$ with known flowrate $F_2$ (Eq. E.1). This is similar to a type of nonlinear feedforward (ratio) control.

$$z_2 = \frac{k_{v1}}{k_{v2}} z_1 \tag{E.1}$$

where $k_{v1}$ and $k_{v2}$ are given in Table A.2.

Then, we can update the internal PI-controller bias ($v_0$) by adding to it the value

$$\Delta v = v(z_2) - v(z_1) \tag{E.2}$$

where $v(z_1)$ and $v(z_2)$ are the values of the output ($v$) of the internal PI-controller in SRC for the two valve positions ($z_1$ and $z_2$), for example, determined from Fig. E.17 (or the corresponding equations).